Original

Iskhakova, K.; Wieland, D.; Zeller-Plumhoff, B.; Willumeit-Römer, R.:
Utilizing x-ray diffraction tomography to study the effect of biodegradable magnesium implants on the bone ultrastructure.
In: Proc. SPIE : Developments in X-Ray Tomography XIII. Vol. 11840 2021. 118400M.

First published online by SPIE: 09.09.2021

https://dx.doi.org/10.1117/12.2593704

Utilizing X-ray diffraction tomography to study the effect of biodegradable magnesium implants on the bone ultrastructure

Kamila Iskhakova[a], D.C. Florian Wieland[a], Berit Zeller-Plumhoff[a], Regine Willumeit-Römer[a]
[a]Institute of Metallic Biomaterials, Helmholtz-Zentrum hereon GmbH, Max-Planck-Straße 1, 21502 Geesthacht, Germany

ABSTRACT

Magnesium-based alloys are suitable materials for biodegradable bone implants due to their high biocompatibility and mechanical properties similar to bone. Diffraction tomography (DCT) is an imaging technique based on acquiring position-resolved diffraction patterns at multiple angular orientations. DCT is able to provide information about the crystal structure of hydroxyapatite (HAp) in bone, which is necessary for understanding the influence of magnesium degradation on the bone tissue. This article presents a study of a sheep bone explant containing a biodegradable magnesium-zinc-calcium (BRI.Mag, Mg-Zn-Ca) alloy implant. The DCT data were reconstructed and analyzed using the MATLAB computing environment and ASTRA Toolbox. Thus, the DCT images with 200 µm pixel size were reconstructed, and, therefore, a DCT study workflow was developed. That allowed to retrieve the crystal lattice parameters of HAp such as full width at half maxima (FWHM) and reflection position around the implant surface of a selected (002) diffraction peak. Based on these parameters, the corresponding d-spacing and crystal size of HAp were determined. It was shown that the degradation of the implant does not notably affect the lattice spacing of the bone within a distance of 3 mm from the implant surface. At the same time, the crystal size decreases closer to the implant (1.5 mm). The developed workflow for the reconstruction of a volume-resolved diffraction experiment of a bone explant containing metal implants is a convenient approach to investigate the crystal structure of the sample on exact locations in a non-invasive way. The workflow will be further applied for a broader range of samples containing Mg-based biodegradable implants.

Keywords: X-ray diffraction tomography, biodegradable implant, Mg-Zn-Ca implant, bone ultrastructure

1. INTRODUCTION

Magnesium (Mg)-based biodegradable implants gained high attention in recent years. Due to high biocompatibility and good mechanical properties similar to the bone itself, Mg-based implants are suggested to be a beneficial tool in bone fracture treatment. The major advantage of such biodegradable implants is that they can degrade in the body and do not require surgical intervention for removal. This is more favorable for patient safety and lifts a part of the financial load from the healthcare system. Moreover, depending on the alloying elements, the properties of an Mg-based alloy, such as degradation rate and strength, can be tailored with respect to the application [1]. Alloying magnesium with calcium (Ca) and zinc (Zn), for instance, is reported to increase the biocompatibility and mechanical properties of the implant [2].

To progress in the development of Mg-based implants, it is crucial to attain an in-depth understanding of the tissue reorganization following implantation and the incorporation of the implant into the bone matrix. Research on Mg-based implants has mostly focused on mechanical properties, degradation kinetics and inflammatory reactions, or bone growth [3]. Meanwhile, studies on the bone ultrastructure reaction are performed less often despite the high importance of the regeneration process and bone reaction to the implant and its degradation. Bone is a hierarchically structured composite material. There, the lowest level or the ultrastructure is presented by collagen fibrils and hydroxyapatite (HAp) platelets [4]. In order to understand how bone tissue reacts to implant degradation, it is necessary to study how the bone ultrastructure changes during healing [3].

During the healing process, the ultrastructure of a newly formed bone can be affected by implant degradation, e.g., ionic substitution or crystal structure defects. Due to this, the mechanical properties of the bone matrix might change, resulting in worse performance and, thus, failure of the implant. Previous studies, presented by Grünewald *et al*., showed the decrease in HAp platelet size and the platelet thickness in the areas with higher Mg concentrations, as well as the change of HAp platelets' preferred orientation near an implant [5, 6]. Similarly, Zeller-Plumhoff *et al.* reported a decrease in crystal size near the implant area. While the d-spacing had the same values in the area near the implant (trabecular bone) and further (cortical bone) [3].

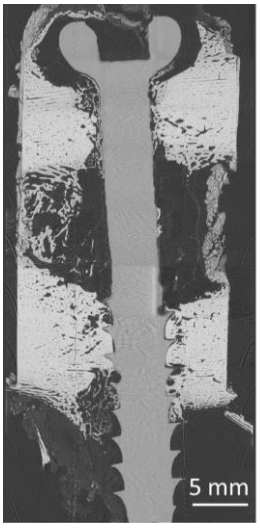

Figure 1. µCT image of a sample containing the sheep bone femur explant and the BRI.Mag implant in the center.

The X-ray diffraction (XRD) study of HA can provide knowledge about ultrastructural parameters. These are namely the bone crystal structure, changes in crystal parameters over time and with respect to the implant material, as well as possible atomic substitutions and positions of preferred substitution in the crystal lattice. However, commonly used 2D XRD studies are limited to a slice from the sample and cannot provide the bulk information. Diffraction computed tomography (DCT), on the other hand, allows us to learn about the bone ultrastructure in the 3D volume by acquiring position-resolved diffraction data at many angular orientations of a sample [7]. Nevertheless, the amount of studies of bone with the use of DCT is limited. There were several DCT studies of bone samples performed in the last years. One was the study of a human bone with the resolution down to 120 nm with a beamsize around 30 × 30 nm^2 [8], and the second was the study of bone fossils with a beamsize of 20×20 μm^2 and voxel size of 150 µm [9]. Up to this day, no DCT study of bone explants containing a biodegradable implant has been performed. Therefore, the aim of this study was to develop and optimize the workflow of the DCT study of a bone explant containing biodegradable metal implant.

2. MATERIALS AND METHODS

2.1 Bone explant preparation

The screw-shaped implant made of BRI.Mag alloy (Mg-Zn-Ca) was implanted into the sheep tibia. The animal trial was approved by the Austrian Federal Ministry for Science and Reasearch (Permit Number: BMWF-66.010/0017-II/3b/2014). The screws had a size of 5 mm in diameter and 20 mm in length. After six weeks of healing, the sheep was sacrificed, and the bone explant containing the implant was extracted. In order to preserve the explant, the sample was critical point dried. The resulting overall size of the sample was 10 x 20 mm. The reconstructed micro-computed tomography (µCT) image of the sample, obtained at P05 endsation at PETRA III storage ring at Deutsches Elektronen-Synchrotron (DESY, Hamburg, Germany), is shown in Figure 1.

2.2 X-ray diffraction tomography experiment

X-ray diffraction tomography was performed at the P07 side station at the PETRA III (DESY, Hamburg, Germany). An X-ray beam with energy at 87.1 keV was utilized, and the beam size was set to 0.2 mm in horizontal and vertical directions by slits. A 2D slice in the plane orthogonal to the screw axis was scanned with a 0.2 mm step size. The sample was mounted on a rotation stage to capture projections over 180° at an angular step size of 3° and an exposure time of 0.5 s. As a result, 4026 XRD projections with the resolution of $\Delta q = 0.006$ $Å^{-1}$ were obtained. A Perkin Elmer XRD 1621 flat panel detector (PerkinElmer, Waltham, US) was placed at a 1.485 m distance from the sample. For the data calibration, lanthanum hexaboride (Lab6) was used.

2.3 Data reconstruction

For the data reconstruction, we have followed the sequence shown in Figure 2. The parameters for the data calibration were determined by the DAWN 2.18.0 software suit (Diamond Light Source, Didcot, UK). That step was followed by XRD radial integration performed by using the DAWN software. The data was normalized to account for beam intensity and the sample

thickness on the basis of the transmitted beam intensity determined by the active beamstop for each measured sample position. From the normalized diffractograms, the XRD reflections from the 002 planes of HAp and Mg were selected for further processing as both peaks had a significant peak intensity and did not overlap with the peaks coming from the other material (Mg and HAp, respectively). In the next step, the sinogram of the XRD reflection was created, and the DCT images were reconstructed. The reconstruction algorithm was created with the use of the ASTRA Toolbox version 1.9 for 2D and 3D tomography. For the tomographic reconstruction, the Conjugate Gradient Least Squares (CGLS) algorithm was used, as it was proven to be effective in application to tomographical reconstructions [10, 11]. As a next step, a Gaussian fitting with the use of the Matlab function "fminsearch" was executed. The fitting was computed utilizing the MATLAB R2018a (The MathWorks, Inc., Natick, US) computing environment. By fitting a Gaussian, three parameters of the XRD signal were extracted: peak intensity I, full width at half maximum (FWHM), and the peak position (q). Additionally, a mask cutting out the sample background was applied in order to remove reconstruction artifacts around the sample surface.

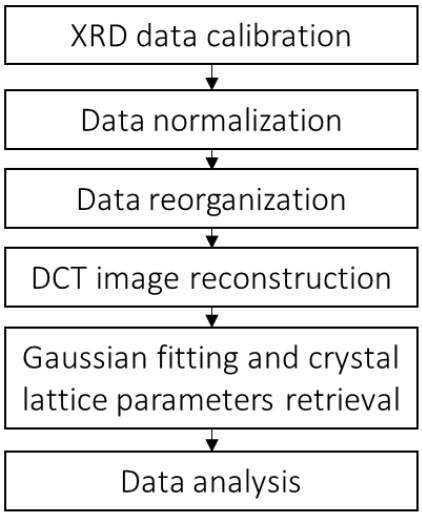

Figure 2. The flow chart representing the DCT data analysis workflow developed and optimized in application to the sheep bone explant containing the biodegradable Mg-10Gd implant. The workflow starts with XRD data calibration and normalization, followed by conversion of the data into the sinograms. After that, an image is being reconstructed. Later, a Gaussian fitting is applied to obtain lattice parameters, such as crystal size and d-spacing. How do those parameters change with a distance from an implant is then analyzed.

2.4 Crystal lattice parameters

In order to calculate the bone ultrastructure parameters on the basis of retrieved FWHM and q, the following approach was employed. The Bragg's law, stating $n\lambda = 2d\sin\theta$, was used to calculate the d-spacing. There n is the diffraction order, λ is the X-ray beam wavelength, and θ is XRD reflection position. To calculate the crystal size, the Scherrer equation was utilized. Scherrer equation states that crystal size is equal to $\tau = K\lambda/(FWHM \times \cos\theta)$, where K is a shape factor.

3. RESULTS AND DISCUSSION

With the reconstruction approach described above, a 2D cross-section of the sheep bone explant containing bone tissue and the Mg-Ca-Zn screw after six weeks of healing was imaged. Figure 3 displays two different reconstructed X-ray diffractograms obtained from the bone and the implant area, respectively. The reconstructed diffractogram from the screw area shows a significant increase in Mg reflections intensity.

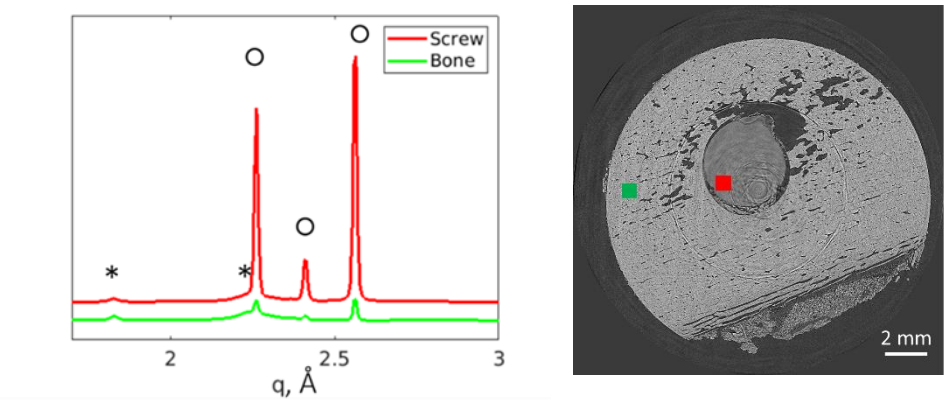

Figure 3. The reconstructed X-ray diffractograms (left) obtained from the voxels belonging to the screw (red) and bone (green). The HAp reflections (*) seem to maintain the same intensity, while the Mg reflections (○) are significantly more pronounced in the screw. Red and green rectangles on the µCT (right) identify the regions in which the reconstructed diffractograms were obtained.

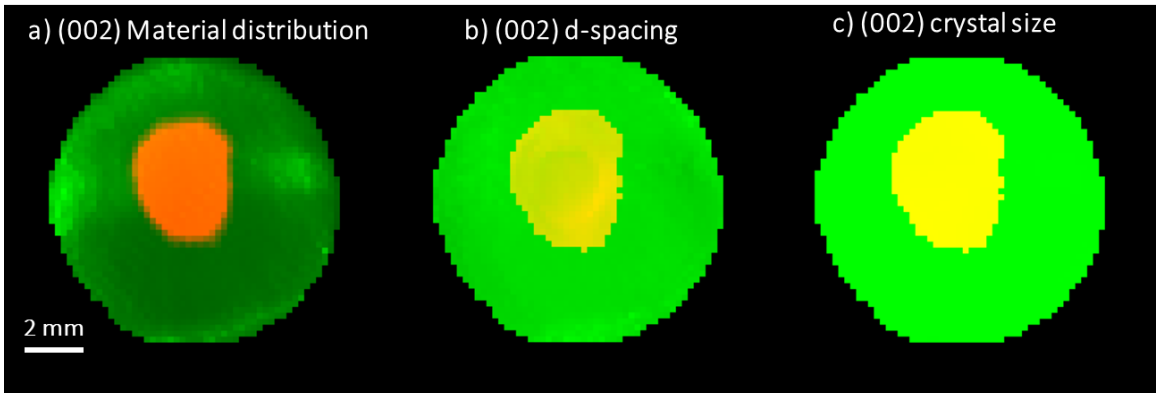

Figure 4. False-colored DCT imagest of the explant containing Mg-10Gd screw (orange is implant, green is bone). a) material distribution map, b) d-spacing map, c) crystal size map, with a voxel size of 200 µm.

Three parameters were obtained on the basis of the reconstruction of the XRD reflections: the peak position, the FWHM, and the peak intensity. Based on this, the d-spacing and the crystal size were calculated, while the intensity of the diffraction peaks enabled us to deduce a material distribution map. Figure 4 shows a fake-coloured material distribution, d-spacing, and crystal size maps, where orange represents the screw and green represents the bone. The size of the screw image is slightly bigger than it is on the µCT image, which might be caused by the reconstruction artifacts, which, in turn, complicate the segmentation.

Figure 5 shows the change of the d-spacing and crystal size values for the (002) HAp reflection as a function of the distance from the implant surface. Furthermore, the mean value of the d-spacing for the 002 plane of HAp over the whole sample was

calculated, resulting in a value of 3.437 Å, which corresponds to the literature where a value of 3.437 Å is reported [12]. The average crystal size of 36 nm, as well, corresponds to the reported values of 20-50 nm [13].

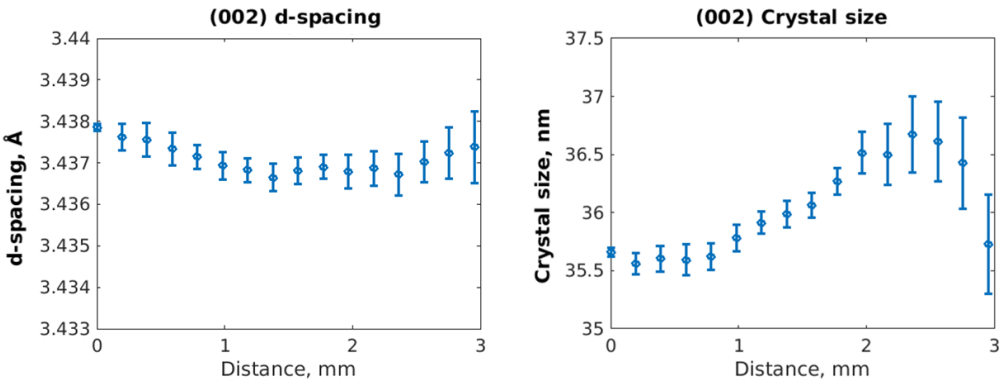

Figure 5. The (002) HAp reflection d-spacing (left) and crystal size (right) values as a function of the distance from the BRI.Mag implant surface. The d-spacing does not show a significant change with the distance from the implant, while the crystal size shows a decrease by approaching the implant interface. The values means and confidence intervals calculated over all voxel.

Furthermore, the d-spacing and the crystal parameters were calculated as a function of the distance from the implant surface over all respective voxels. Figure 5 shows that the d-spacing does not change significantly as a function of the distance from the implant interface. The crystal size, on the other hand, seems to be lower in the area close to the implant (up to 1.5 mm). The study by Zeller-Plumhoff *et al.* focused on magnesium-gadolinium alloys and reported a similar behavior for both d-spacing and crystal size of HAp in trabecular bone (closer to the implant) and cortical bone (further from the implant) [3]. It was suggested that the lower values of crystal size might indicate a higher concentration of Mg, as was shown by Bertoni *et al.* or Grünewald *et al.* [3, 7, 14]. As we observe similar changes in crystal size in the area close to the implant, it would be safe to assume that the bone in that area might contain the increased concentration of Mg.

The obtained result can be refined by increasing the spatial resolution. That might be achieved by choosing smaller scanning and angular steps, as well as smaller beam size, which in turn would result in a longer time required for the measurement.

4. CONCLUSION

The first DCT study on a large animal model explant with an implanted biodegradable Mg screw was performed. The DCT analysis workflow for a bone sample containing a metal implant was developed and optimized. With the use of synchrotron X-radiation, the material distribution, crystal size, and d-spacing maps with 200 µm pixel size were reconstructed. The d-spacing is shown to not be affected by the implant, while the crystal size decrease in the area close to the implant. The DCT approach is revealed to be a convenient method in *ex vivo* studies of a biodegradable metal implant degradation influence on the bone ultrastructure.

ACKNOWLEDGEMENTS

This project has received funding from the European Union's Horizon 2020 research and innovation program under the Marie Skłodowska-Curie grant agreement No. 811226. The authors acknowledge funding from the German Federal Ministry of Education and Research for project MgBone (BMBF project number 05K16CGB). We thank Dr. Emad Maawad (Helmholtz-Zentrum hereon GmbH, Germany) for the help with the DCT experiment and Helmholtz-Zentrum hereon GmbH for providing

the beamtime. We also thank Prof. Annelie-Martina Weinberg and Dr. Nicole Sommer (Medical University of Graz, Austria) for providing the sample.

REFERENCES

[1] Witte, F. Hort N., Vogt, K. Cohen, S. Kainer, K. U., Willumeit-Römer, R., Feyerabend, F., “Degradable biomaterials based on magnesium corrosion”, Curr Opin Solid State Mater Sci 12 (5-6), 63-72 (2008).

[2] J. Hofstetter, M. Becker, et al., High-strength low-alloy (HSLA) Mg-Zn-Ga alloys with excellent biodegradation performance, JOM 66, 566-572 (2014).

[3] Zeller-Plumhoff, B. Malich, C., Krüger, D., Campbella, G., Wiese, B., Galli, S., Wennerberg, A., Willumeit-Römer, R., Wieland, D. C. F., "Analysis of the bone ultrastructure around biodegradable Mg-xGd implants using small angle X-ray scattering and X-ray diffraction", Acta Biomaterialia 101, 637-645 (2020).

[4] Georgiadis, M., Müller, R., Schneider, P., "Techniques to assess bone ultrastructure organization: orientation and arrangement of mineralized collagen fibrils, The Ultrastructure of Bone and Its Relevance to Mechanical Properties", J. R. Soc. Interface.13, 20160088 (2016).

[5] Grünewald, T.A., Ogier, A., Akbarzadeh, J., Meischel, M., Peterlik, H., Stanzl-Tschegg, S., Löffler, J. F., Weinberg, A. M., Lichtenegger, H. C., "Reaction of bone nanostructure to a biodegrading Magnesium WZ21 implant – A scanning small-angle X-ray scattering time study", Acta biomaterialia 31, 448-457 (2016).

[6] Grünewald, T.A., Rennhofer, H., Hesse, B., Burghammer, M., Stanzl-Tschegg, Cotte, M., Löffler, J. F., Weinberg, A. M., Lichtenegger, H. C., "Magnesium from bioresorbable implants: Distribution and impact on the nano- and mineral structure of bone", Biomaterials 76, 250-60 (2016).

[7] Frølich, S., Leemreize, H., Jakus, A., Xiao, X., Shah, R., Birkedal, H., Almerc, J.D., Stockd, S. R., "Diffraction tomography and Rietveld refinement of a hydroxyapatite bone phantom", Journal of Applied Crystallography 49(1), 103-109 (2016).

[8] Palle, J., Wittig, N. K., Kubec, A., Niese, S., Rosenthal, M., Burghammer, M., Grünewald, T. A., Birkedal, H., "Nanobeam X-ray fluorescence and diffraction computed tomography on human bone with a resolution better than 120 nm", Journal of Structural Biology 212 (3), 107631 (2020).

[9] Mürer, F.K., Sanchez, S., Álvarez-Murga, M., Di Michiel, M., Pfeiffer, F., Bech, M., Breiby, D.W., "3D Maps of Mineral Composition and Hydroxyapatite Orientation in Fossil Bone Samples Obtained by X-ray Diffraction Computed Tomography", Sci Rep 8, 10052 (2018).

[10] Hestenes, M. R., Stiefel, E., "Methods of Conjugate Gradients for Solving Linear Systems", Journal of Research of the National Bureau of Standards 49(6), 409-436 (1952).

[11] Kloek, T., Bachelor thesis "Conjugate Gradients and Conjugate Residuals type methods for solving Least Squares problems from Tomography", TU Delft, Deft, Netherlands (2012).

[12] Downs, R.T., Bartelmehs, K.L., Gibbs, G.V., "Interactive software for calculating and displaying X-ray or neutron powder diffractometer patterns of crystalline materials", American Mineralogist 78, 1104-1107 (1993).

[13] Schwarcz, H. P., Abueidda, D., Jasiuk, I., "The Ultrastructure of Bone and Its Relevance to Mechanical Properties", Front. Phys. 5, 39 (2017).

[14] Bertoni, E., Bigi, A., Cojazzi, G., Gandolfi, M., Panzavolta, S., Roveri, N., "Nanocrystals of magnesium and fluoride substituted hydroxyapatite", J Inorg Biochem 72(1-2), 29-35 (1998).